Nuclear Materials and Energy 27 (2021) 100982

Contents lists available at ScienceDirect

Nuclear Materials and Energy

journal homepage: www.elsevier.com/locate/nme

Comparison of a collisional-radiative fluid model of H_2 in UEDGE to the kinetic neutral code EIRENE

A. Holm [a,b,*], P. Börner [c], T.D. Rognlien [a], W.H Meyer [a], M. Groth [b]

[a] Lawrence Livermore National Laboratory, Livermore, CA 94550, USA
[b] Aalto University, P.O.Box 11000, FI-00076 AALTO, Finland
[c] Institut für Energie- und Klimaforschung - Plasmaphysik, Forschungszentrum Jülich GmbH, 52425 Jülich, Germany

ARTICLE INFO

Keywords:
Collisional-radiative model
Hydrogen molecules
Fluid model
UEDGE
EIRENE
Molecules

ABSTRACT

A fluid collisional-radiative model for H_2 has been implemented in the edge-fluid code UEDGE and compared to the kinetic neutral code EIRENE on a simple, 2D, orthogonal domain with a constant, static plasma distribution. The novel CRUMPET Python tool was used to implement dissociation and energy rate coefficients that consider molecular-assisted processes, binding energy, and radiation due to molecular processes into the UEDGE fluid molecular model. The agreement between the fluid and kinetic molecular models was found to be within 20% when corresponding rates were used in UEDGE and EIRENE for a domain with absorbing boundaries. When wall recycling was considered, EIRENE predicted up to a factor of 2.2 higher molecular densities than UEDGE at $T < 5$ eV. The difference is due to the absence of radial gradients driving diffusive wall fluxes and, thus, recycling in UEDGE and molecular self-scattering in EIRENE, and is likely dependent on plasma profiles and domain geometry. Comparison of the molecular energy sources in EIRENE and UEDGE suggest the constant elastic scattering rate coefficient used in UEDGE needs to be updated to a temperature-dependent coefficient and that atom-molecule equipartition should be considered in the EIRENE model for background plasma density in excess of $1 \times 10^{19} m^{-3}$. Finally, collisional-radiative CRUMPET simulations indicate that the vibrational molecular populations become comparable to the ground-state molecular population when the plasma temperature decrease below 6 eV and, thus, require time-dependent evaluation.

1. Introduction

Under detached conditions in diverted fusion devices, plasma temperatures are sufficiently low for significant molecular populations to form in the plasma, especially in carbon devices as the target fluxes preferentially recycle as molecules on graphite targets [1]. For electron temperatures, T_e, below 3 eV, which coincide with the experimentally observed onset of detachment [2], molecules undergo reaction chains that affect the divertor power and particle balance. These processes include electronic, vibrational, and rotational excitation and relaxation, as well as molecular-assisted recombination, dissociation, and ionization processes (MAR, MAD, and MAI, respectively) [3,4].

Kinetic neutral codes, such as EIRENE [5] and DEGAS2 [6], are widely used to assess the atomic and molecular populations and are coupled to fluid edge-plasma codes to simulate divertor plasmas. However, the computational time for kinetic codes increases exponentially with increasing collisionality, and the predictions have inherent statistical noise, making it challenging to assess whether a steady-state solution is achieved. Additionally, at high neutral densities when neutral self-scattering becomes significant, the system becomes non-linear, necessitating iterative simulations to achieve steady-state solutions. Under such conditions, either high-performance computing is necessary to perform kinetic simulations in a timely manner or fluid atomic and molecular models can be utilized. Fluid models are expected to yield better predictions when neutral self-scattering is significant, as they are well-suited for solving non-linear systems, achieve numerical convergence, and have shorter computational times than kinetic models. Fluid models assume the atom and molecular mean-free paths to be significantly shorter than the characteristic size of the system, which is typically violated at high plasma temperatures and low densities. Under such conditions, hybrid fluid-kinetic models [7] can be utilized to improve the accuracy of the fluid model via kinetic correction terms. The decrease in runtime of hybrid models compared to fully kinetic simulations depends on the accuracy of the fluid solution, calling for

* Corresponding author.
E-mail address: andreas.holm@aalto.fi (A. Holm).

https://doi.org/10.1016/j.nme.2021.100982
Received 28 August 2020; Received in revised form 3 March 2021; Accepted 17 March 2021
Available online 26 March 2021

Table 1
List of reactions included in CRUMPET. Here, n denotes the electronical state of the atoms, and v denotes the vibrational state of the molecules. Unless an excited state is mentioned for a molecular or atomic species, it is at its ground state. Reactions marked with † are reactions corresponding to those considered in the EIRENE Kotov-2008 model.

	Reaction	Ref	Reaction	Ref
	$e^- + H_2 \rightarrow e^- + H\left(EF^1\Sigma_g^+\right)$	[13]	$e^- + H^- \rightarrow 3e^- + p^+$	[13]
	$e^- + H_2 \rightarrow e^- + H\left(a^3\Sigma_g^+\right)$	[13]	$p^+ + H^- \rightarrow p^+ + e^- + H$	[13]
	$e^- + H_2 \rightarrow e^- + H + H(n = 2)$	[13]	$p^+ + H^- \rightarrow H + H(n = 2)$	[13]
†	$e^- + H_2(v) \rightarrow e^- + 2H$	[14]	$p^+ + H^- \rightarrow H + H(n = 3)$	[13]
	$e^- + H_2 \rightarrow e^- + 2H(n = 2)$	[13]	$e^- + H_2(v) \rightarrow e^- + H_2(v \pm 1)$	[14]
	$e^- + H_2 \rightarrow e^- + H + H(n = 3)$	[13]	$H^*(n > 1) \rightarrow H^*(n' < n)$	[15]
†	$e^- + H_2(v) \rightarrow 2e^- + H_2^+$	[14]	$e^- + H_2(v) \rightarrow e^- + H_2\left(B^1\Sigma_u^+\right)$	[12]
†	$e^- + H_2 \rightarrow 2e^- + p + H$	[13]	$e^- + H_2(v) \rightarrow e^- + H_2\left(C^1\Pi_u\right)$	[12]
†	$e^- + H_2^+ \rightarrow 2e^- + 2p$	[13]	$e^- + H_2\left(EF^1\Sigma_g^+\right) \rightarrow e^- + H_2\left(B^1\Sigma_u^+\right)$	[16]
†	$e + H_2^+ \rightarrow e + p + H$	[13]	$H_2\left(a^3\Sigma_g^+\right) \rightarrow H_2\left(b^3\Sigma_u^+\right) \rightarrow 2H$	[16]
	$e + H_2^+ \rightarrow e + p + H(n = 2)$	[13]	$H_2\left(c^3\Pi_u\right) \rightarrow H_2\left(b^3\Sigma_u^+\right) \rightarrow 2H$	[17]
†	$e^- + H_2^+ \rightarrow H + H(n = 2 - 8)$	[18]	$H_2\left(B^1\Sigma_u^+\right) \rightarrow H_2(v)$	[12]
	$e^- + H_2(v) \rightarrow H + H^-$	[14]	$H_2\left(C^1\prod_u\right) \rightarrow H_2(v)$	[12]
†	$p^+ + H_2(v) \rightarrow H_2^+ + H$	[14]	$H_2\left(B^1\Sigma_u^+\right) \rightarrow 2H$	[12]
	$p^+ + H_2 \rightarrow p^+ + H_2^+ + e^-$	[13]	$H_2\left(C^1\prod_u\right) \rightarrow 2H$	[12]
	$p^+ + H_2^+ \rightarrow 2p^+ + H$	[13]	$e^- + H_2(v) \rightarrow e^- + H_2\left(c^3\Pi_u\right)$	[16]
	$e^- + H^- \rightarrow 2e^- + H$	[13]	$e^- + H^*(n > 1) \rightarrow 2e^- + p^+$	[18]

accurate fluid models of atoms and molecules.

This work implements effective collisional-radiative reaction rates for hydrogen molecules, H_2, into the fluid molecular model of the multi-fluid edge code UEDGE [8]. The results of the model are compared to kinetic neutral predictions by EIRENE to assess the accuracy of the fluid molecular model compared to a kinetic molecular model.

2. Implementation of a fluid H_2 model in UEDGE using collisional-radiative CRUMPET rate coefficients

The large number of electronic, vibrational, and rotational molecular states and their associated reactions necessitate the application of a collisional-radiative model (CRM), which significantly reduces the dimensionality of the system in order for it to be computationally solved. Specifically, CRMs are used to calculate the effective reaction rate coefficients of a small subset of species, which are simulated time-dependently: herein referred to as P-species. Reactions between a time-dependent P-species and the background plasma produce a combination of plasma species, other time-dependent P-species (e.g. $e^- + H_2 \rightarrow 2e^- + p^+ + H$, where H and H_2 both are P-species) and "conduit" species, which will undergo further reactions with the background plasma (e.g. $e^- + H_2 \rightarrow 2e^- + H_2^+$, where H_2^+ is a "conduit" species). Such "conduit" species, herein referred to as Q-species, have short lifetimes and will readily undergo further reactions, preventing the buildup of density of such Q-species. These reactions eventually yield a background plasma or P-species (e.g. $e^- + H_2^+ \rightarrow e^- + p^+ + H$): thus, the effective reaction rate coefficients of the P-species are dependent on the reaction rate coefficients of reactions involving Q-species. CRMs have been widely applied to atomic processes, where the choice of P- and Q-species is dependent only on the species lifetime. However, in molecular CRMs there are additional criteria for choosing the optimal P- and Q-species, which depend on the plasma temperature, density, as well as the states and reactions included in the CRM [9,10].

This work uses a novel Python tool, the Collisional-Radiative UEDGE Model for Plasma Edge Theory (CRUMPET) [11], to construct and assess a Greenland-type CRM [12] for H_2. The Greenland-type CRM is applicable to systems with competing radiative and collisional processes, where the P- and Q-species interact with the plasma background but not with one another. By design, CRUMPET is only limited by the availability of reaction rate coefficients, while the user is allowed to define the P-, Q-, and background plasma species to be considered.

CRUMPET is used to create a CRM for electronically and vibrationally resolved hydrogen molecules, including all reactions in Table 1. The P-space consists of ground state atoms (H) and molecules in their electronical and vibrational ground state (H_2), and the Q-space consists of vibrationally excited molecules in their electronic ground state ($H_2(v = 1–14)$), electronically excited atoms up to n = 8 (H(n = 2–8)), electronically excited molecular singlet and triplet states up to n = 2 (H_2(X), where X specifies the electron state), molecular ions (H_2^+), and negative ions (H^-). Presently, no vibrational states of the electronically excited molecules are considered in the model. The energy of the species in the P- and Q-space, which is used to calculate the reaction rate of proton-impact reactions, is taken to be E = 0.1 eV, due to the availability of AMJUEL data used in this work [18]. The molecular initial energy is not expected to affect the effective rates evaluated by CRUMPET, as they display a negligible dependence on the P- and Q-species energy for E < 5 eV, but such effects may become important for particle and energy transport, which is not evaluated by CRUMPET. The choice of P-space is motivated by the present implementation of the atomic and molecular model in UEDGE. The validity of this CRM has not been assessed by the criteria outlined in [9,10], and no attempt has been made to identify the optimal P-space for the conditions investigated. The plasma background consists of ionic hydrogen and electrons and is assumed to be thermally equilibrated ($T_e = T_i$) with effective charge state $Z_{eff} = 1$ ($n_e = n_i$). The validity of these assumptions was assessed and are considered valid for high-density ($n_e > 1 \times 10^{19}$ m^{-3}), low-temperature ($T_e < 5$ eV) plasmas, such as detached divertor plasmas. The data in [13,14,18] are only valid for $T_e > 0.5$ eV: for lower temperatures linear interpolation between zero and the rate coefficient at $T_e = 0.5$ eV is applied.

The CRUMPET model implemented in UEDGE does not consider atomic ionization or three-body/radiative recombination of plasma ions, which are calculated by UEDGE. Rather, CRUMPET simulates H_2 until the reaction products are either a ground-state atom or an ion and writes n_e- and T_e-dependent tables of the effective rate coefficients for the H source and H_2 sink that are read by UEDGE. UEDGE then solves the time-dependent continuity equation, including transport of H and H_2, for every grid cell at each increasing time steps until a fully converged

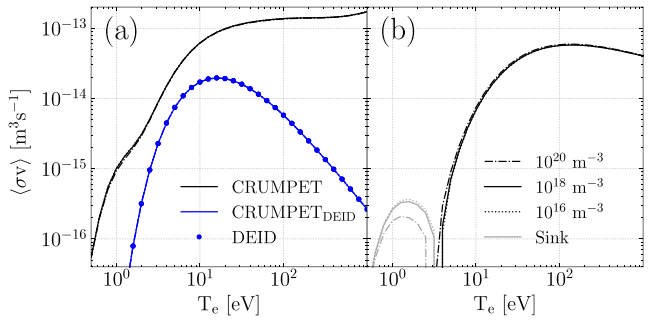

Fig. 1. CRUMPET (black) atom (a) and ion (b) particle rate coefficients as a function of electron temperature for plasma densities 1×10^{20} m^{-3} (-.), 1×10^{18} m^{-3} (–), and 1×10^{16} m^{-3} (…) as calculated by CRUMPET. The faint lines in (b) are sink terms, mirrored in the ordinate. Also shown is the DEID rate used in the previous UEDGE model (●) together with the corresponding rate coefficients as calculated by CRUMPET (–). Here, $T_e = T_i$ and $n_e = n_i$ is assumed.

steady-state at computer precision is achieved, as assured by evaluating a time-step $dt \to \infty$ in the implicit solver.

The CRUMPET molecular CRM predicts H source rate coefficients $\langle\sigma v\rangle_{\mathrm{H2}\to\mathrm{H}}$ [m^{3}s^{-1}] in excess of one and two orders of magnitude larger than the previously implemented UEDGE model for $T_e > 30$ eV and $T_e < 1$ eV, respectively (Fig. 1a). The previous fluid molecular model in UEDGE assumed direct electron-impact dissociation (DEID), $e^- + H_2 \to e^- + 2H(n=1)$ (2.2.5 in [18]), to be the sole dissociation process. CRUMPET was used to calculate the rate coefficients of this DEID-only model (CRUMPET$_{\mathrm{DEID}}$), which agree exactly with the DEID rates coefficients, validating the CRUMPET implementation (Fig. 1a).

The CRUMPET model introduces an ion sink/source rate coefficient $\langle\sigma v\rangle_{\mathrm{H2}\to\mathrm{i}}$ [m^{3}s^{-1}] that captures the effects of MAR, MAD, and MAI, which are not considered by the DEID-only model (Fig. 1b). MAR occurs for $T_e \lesssim 3.5$ eV, when proton-impact processes become significant (Fig. 1b, grey lines). However, $\langle\sigma v\rangle_{\mathrm{H2}\to\mathrm{i}}$ is small compared to $\langle\sigma v\rangle_{\mathrm{H2}\to\mathrm{H}}$ (Fig. 1): thus, it is expected that the inclusion of molecular-assisted processes will affect the plasma state for 1 eV $< T_e <$ 5 eV, when both recombination and ionization rates are small. Both $\langle\sigma v\rangle_{\mathrm{H2}\to\mathrm{i}}$ and $\langle\sigma v\rangle_{\mathrm{H2}\to\mathrm{H}}$ display a weak dependence on plasma density for $T_e > 3.5$ eV.

CRUMPET also solves the energy source and sink terms associated with molecular processes for the ions, electrons, atoms, radiation, and potential in terms of energy rate coefficients $\langle\sigma vE\rangle$ [Jm^{3}s^{-1}]. Here, CRUMPET conforms to the UEDGE assumption of a common temperature for ions and atoms and, thus, calculates the combined ion/atom energy rate coefficient $\langle\sigma vE\rangle_{i/a}$. For the applied model the potential energy rate coefficient reduces to the molecular binding energy rate coefficient $\langle\sigma vE\rangle_{bind}$, as H and H_2 are the only P-species. The radiation rate coefficient is split into the contribution of molecular lines $\langle\sigma vE\rangle_{H2-rad}$, and atomic lines $\langle\sigma vE\rangle_{H-rad}$ due to exited atoms created by molecular processes: both contributions need to be scaled by the electron and H_2 densities to assess the net radiated power due to molecular processes.

The energy rate coefficients are calculated in a manner analogous to that for the electrons in [12]:

$$\dot{\varepsilon}_k^{i/a} = \sum_{i,j} \Delta_{ij}^k R_{ij}^k(T) n_i n_j, \tag{1}$$

$$\dot{\varepsilon}_k^{bind} = -\sum_{i,j} (E_j - E_k) R_{ij}^k(T) n_i n_j - n_k \sum_j (E_k - E_j) A_k^j, \tag{2}$$

$$\dot{\varepsilon}_k^{rad} = n_k \sum_j (E_k - E_j) A_k^j \ , \tag{3}$$

where $\dot{\varepsilon}_k$ is the rate of change in energy for the ion/atom sink/source (Eq. 1), the potential energy sink/source (Eq. 2), and the radiation source for species $k \in \mathrm{P} \cup \mathrm{Q}$ (Eq. 3), respectively. Here, $R_{ij}^k(T)$ are the

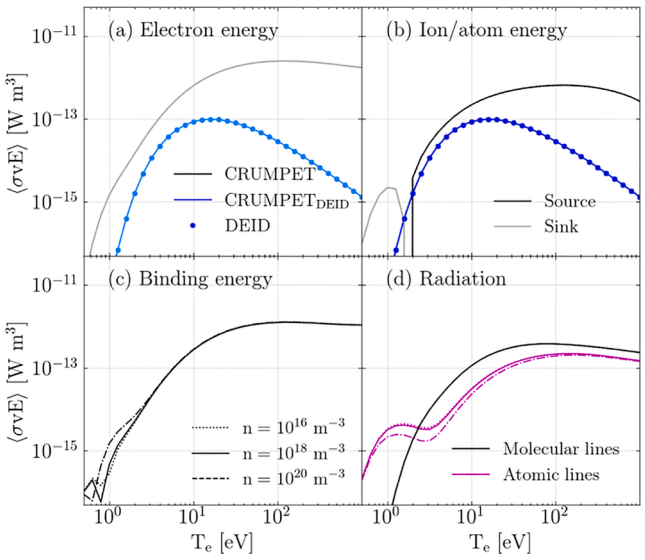

Fig. 2. The electron (a), ion/atom (b), binding (c), and radiation (d) rate coefficients as a function of electron temperature for plasma densities 1×10^{20} m^{-3} (-.), 1×10^{18} m^{-3} (–), and 1×10^{16} m^{-3} (…) as calculated by CRUMPET. The faint lines in (a) and (b) are sink terms, mirrored in the ordinate, and the radiation is split into atomic (–) and molecular (–) lines (d). Also shown are the energy rates used in the previous DEID-only UEDGE model (●) together with the corresponding CRUMPET-evaluated rates (–). Here, $T_e = T_i$ and $n_e = n_i$ is assumed.

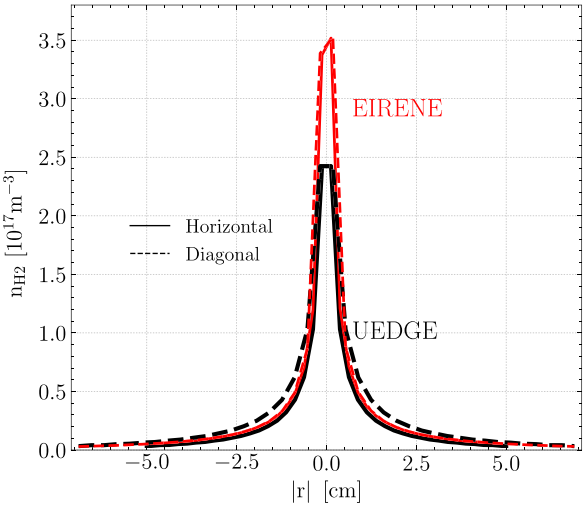

Fig. 3. Horizontal (–) and diagonal (- -) H_2 density profiles as a function of the distance from the domain center |r| predicted by UEDGE (black) and EIRENE (red) for background plasma density $n_e = 1 \times 10^{18}$ m^{-3} and temperature $T_e =$ 10 eV.

temperature-dependent reaction rate coefficients for reactions where background species i reacts with $j \in \mathrm{P} \cup \mathrm{Q}$ to produce species k and A_k^j the Einstein-coefficients describing spontaneous decay of species k into species j. Further, Δ_{ij}^k is the kinetic energy of the reaction products, which has positive sign for electron-impact processes and negative for proton-impact processes, and E_j is the potential of species j, which can belong to the plasma-, P-, or Q-species. Here, the values of Δ_{ij}^k are taken from [19] and the electron energy sink/source term is calculated from the aforementioned terms by assuming energy conservation.

CRUMPET predicts a cutoff for ion/atom heating at $T_e \sim 2$ eV, due to high proton-impact reaction rates, during which the ions supply both the

binding energy and the kinetic energy of the reactants (Fig. 2b), an effect that is not captured by the DEID-only model. Apart from this effect, the DEID-only model, which uses the default values of 10 eV electron energy loss for each dissociation reaction and 5 eV supplied to each of the resulting atoms, severely underestimates $\langle \sigma v E \rangle_e$ and $\langle \sigma v E \rangle_{i/a}$ compared to CRUMPET (Fig. 2a,b).

The CRUMPET model predicts 60%-70% of the molecule-induced electron energy losses to be carried as binding energy for $T_e > 2.2$ eV and $T_e > 1.2$ eV at $n_e = 1 \times 10^{16}$ m^{-3} and $n_e = 1 \times 10^{20}$ m^{-3}, respectively (Fig. 2). The binding energy, which is not considered by the DEID-only model, may be significant when considering the plasma power balance in fusion reactors, as it cannot be measured spectroscopically. However, since $P_{bind}^{tot} = E_{bind} n_e n_{H2} \langle \sigma v \rangle_{bind}$, the total power carried as binding energy is proportional to the H_2 density, which typically only is significant under detached conditions.

For $T_e < 2.2$ eV and $T_e < 1.2$ eV at $n_e = 1 \times 10^{16}$ m^{-3} and $n_e = 1 \times 10^{20}$ m^{-3}, respectively, the molecule-induced plasma energy losses are mainly radiation, dominated by the atomic lines (Fig. 2c,d). The atomic line radiation peaks at ~ 98% of the molecule-induced plasma energy loss at $T_e = 0.6$–0.8 eV, whereas the molecular line radiation peaks at ~ 30% of the molecule-induced plasma energy loss at $T_e = 3.9$ eV. However, the molecule-induced radiative losses are expected to be a small fraction of the net radiated plasma power since this contribution, analogous to the binding energy, is proportional to the H_2 density, which is expected to be significant under detached conditions only. The molecule-induced excited atom population is driven by proton-impact processes, which peak at $T_e \approx 1.5$ eV (Fig. 2), explaining why atomic radiation is dominant at $T_e < 2$ eV.

3. Assessing the molecular continuity equation in UEDGE using EIRENE

A 0.1 m × 0.1 m × 1 m plasma domain, isotropic in the third dimension, with 100% absorbing walls was simulated in UEDGE and EIRENE to compare the fluid and kinetic molecular models. The domain was assigned a static, flow-free, pure hydrogen, H, background plasma with spatially constant density ($n_e = n_i$) and temperature ($T_e = T_i$), and recombination reactions were excluded. The work evaluates simulations with background plasma densities 1×10^{17} m^{-3}, 1×10^{18} m^{-3}, and 1×10^{19} m^{-3}. A constant, 1 Ampere-equivalent H_2 source in the center of the domain drives the system. In EIRENE the source is a point-source of 0.1 eV molecules, whereas UEDGE uses a volumetric source with a Gaussian distribution with 0.8 mm half-width that is assigned energy corresponding to the local H_2 temperature. In UEDGE, only diffusive transport of H and H_2 was considered: H and H_2 particle and energy fluxes are limited to their corresponding free-streaming fluxes by scaling the transport coefficients by a factor $\left(1 + \left|q/\alpha q_{fs}\right|^2\right)^{-1/2}$. Here, q is the particle or energy flux and q_{fs} the corresponding free-streaming particle or energy flux, $q_{fs} = n_k v_{fs}$ and $q_{fs} = n_k T_k v_k^{fs}$, respectively, and $v_k^{fs} = \sqrt{T_k / 2\pi m_k}$ the free-streaming velocity, and α the flux-limit coefficient for each flux-limited species j. A flux-limit coefficient of $\alpha = 1$ is used in UEDGE for limiting two-sided Maxwellian fluxes: however, when all domain boundaries are fully absorbing the flux becomes a one-sided stream from the center source to the wall. As the molecular scattering mean free paths ($\lambda_{mfp} \geq 0.2$m) are long compared to the domain size (L = 0.1 m), the molecules will not recover a two-sided Maxwellian distribution through interaction with the plasma before reaching the domain boundary: hence, a flux-limit coefficient of $\alpha = 2$ is applied here to account for one-sided Maxwellian fluxes. The EIRENE simulations use the Kotov-2008 neutral model [20], which includes the reactions marked in Table 1. This EIRENE model applies the CR approximation to each of the molecular-assisted processes individually, whereas CRUMPET simultaneously applies the CRM to all reactions considered.

Initially, only the H and H_2 continuity equations were evolved in UEDGE, with an assigned, spatially constant $T_{H2} = 0.1$ eV and $T_H = T_i$. The H_2 content in the domain, N_{H2}, is determined by:

$$\frac{dN_{H2}}{dt} = S_{source} + S_{diss} + S_{wall}, \tag{4}$$

where $N_{H2} = \int n_{H2} dV$, n_{H2} is the H_2 density, dV the cell volume, S_{source} the central H_2 particle source, $S_{diss} = \int n_{H2} n_e \langle \sigma v \rangle_{diss} dV < 0$ s^{-1} the H_2 volumetric dissociation sink where $\langle \sigma v \rangle_{diss} = \langle \sigma v \rangle_{H2 \to H} + \langle \sigma v \rangle_{H2 \to i}$, and S_{wall} the wall sink/source term determined by the recycling model. Since the simulations are run to steady-state and the domain boundaries are fully absorbing, $S_{wall} = -S_{source} - S_{diss}$ is a sink term (Eq. 4). Representative examples of the horizontal H_2 density profiles horizontally and diagonally through the central source are shown in Fig. 3. Both the UEDGE and EIRENE n_{H2} profiles have the same shape, but the UEDGE densities have a lower peak value due to the finite width of the Gaussian H_2 source. The EIRENE H_2 density profile is only dependent on the distance from the source ($|r|$) whereas the UEDGE densities are dependent on the domain boundary conditions, resulting in a slightly higher H_2 density, and smaller density gradient along the diagonal than in the horizontal direction.

At $T_e = 0.25$ eV, the UEDGE and EIRENE N_{H2} predictions are within 4% for all n_e analyzed, indicating similar transport in both UEDGE and EIRENE as $T_e \to 0$ eV (Fig. 4). At this low-temperature limit, the CRUMPET and EIRENE $\langle \sigma v \rangle_{diss}$ are negligible (Fig. 1) and N_{H2} only depends on the wall sink $S_{wall} = -S_{source}$, assuming steady-state. As the particle source rate is the same for both codes, the similar molecular densities

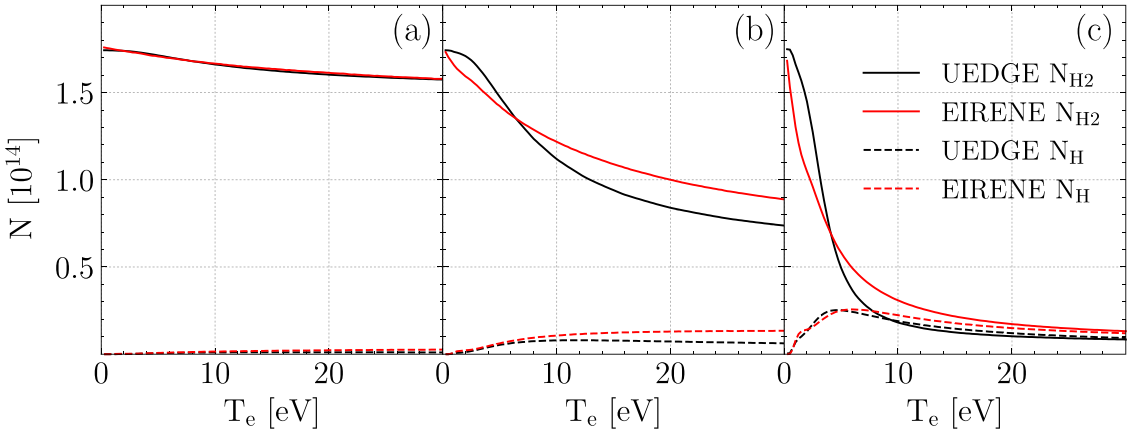

Fig. 4. H_2 (–) and H (–) content as predicted by UEDGE (black) and EIRENE (red) for background plasma densities $n_e = 1 \times 10^{17}$m^{-3} (a), $n_e = 1 \times 10^{18}$ m^{-3} (b), and $n_e = 1 \times 10^{19}$ m^{-3} (c). Here, $T_e = T_i$ and $n_e = n_i$ is assumed.

indicate comparable molecular wall transport, resulting in a comparable wall particle sink, in UEDGE and EIRENE for $T_e \rightarrow 0$ eV.

As the plasma temperature increases, the UEDGE and EIRENE N_{H2} predictions diverge due to the combined effect of the different dissociation rates and molecular transport models in the codes (Fig. 4). UEDGE considers additional molecular reactions compared to the Kotov-2008 model implemented in EIRENE (Table 1), resulting in UEDGE predicting lower N_{H2} for $T_e > 6$ eV and $T_e > 4$ eV for $n_e = 1 \times 10^{18}$ m^{-3} and $n_e = 1 \times 10^{19}$ m^{-3}, respectively. Since $S_{diss} \propto n_e$, the cross-over is determined by the plasma density, occurring at lower T_e as n_e is increased, which also explains why the difference between UEDGE and EIRENE for $n_e = 1 \times 10^{17}$ m^{-3} is negligible. The diffusive molecular transport in UEDGE depends on the density gradients and the constant ion–molecule and atom-molecule elastic scattering rate coefficients $K_{el}^{i-H2} = K_{el}^{H-H2} = 5 \times 10^{-16}$m^{3}s^{-1} [21], whereas the EIRENE model considers ballistic transport with temperature-dependent ion–molecule scattering rates. Thus, the difference in molecular content is affected by both the elastic scattering and dissociation rates.

The lower N_H predicted by UEDGE compared to EIRENE indicate higher ionization rates in UEDGE than in EIRENE (Fig. 4). The atom content in UEDGE is determined by the combined effect of the atom source due to dissociation and recombination, the ionization sink, and atom flux over the absorbing domain boundary which depends on atomic transport. Since recombination is excluded from these simulations, the UEDGE dissociation rate is higher compared to EIRENE, and UEDGE diffusive atom transport to the wall is assumed to be smaller than the ballistic transport in EIRENE, the smaller N_H in UEDGE must be caused by stronger ionization. Assessing the difference in the ionization rates between the codes, and the effects of volumetric recombination, is outside the scope of this work, but should be further pursued.

The extended CRUMPET rates (all reactions in Table 1) are a factor of 2.2 higher than the Kotov-2008 rates (only reactions marked in Table 1) for $T_e > 6$ eV, and similar for $T_e = 1$ eV (Fig. 5) when calculated by CRUMPET. The difference in rates as $T_e \rightarrow 0$ eV is exaggerated, since it is expected that $\langle \sigma v \rangle_{diss} \rightarrow 0$ m^{3}s^{-1} at the low-temperature limit. However, the difference in $\langle \sigma v \rangle_{diss}$ is larger by a factor of 5.5 when calculating the effective rate coefficients from the molecular particle sinks in UEDGE and EIRENE. The additional factor of 2.5 discrepancy is due to differences between transport and the CRM application in EIRENE compared to UEDGE (Fig. 5).

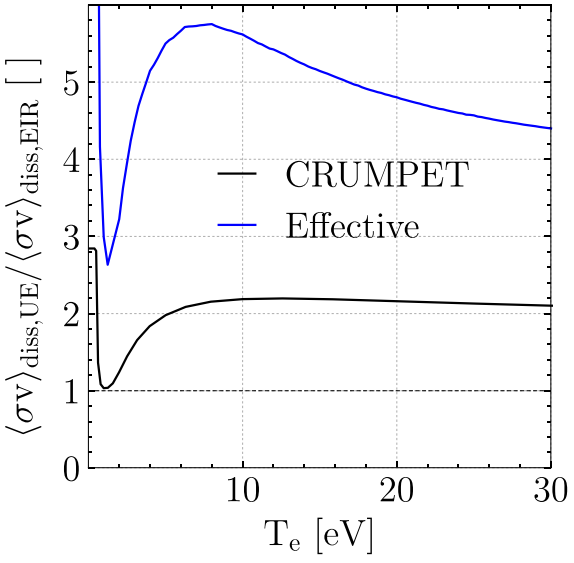

Fig. 5. The ratio of the extended CRUMPET dissociation rates implemented in UEDGE to the Kotov-2008 rates used in EIRENE as evaluated by CRUMPET according to Table 1 (–) along with the ratio of the effective rates from the UEDGE and EIRENE simulations (–) for $n_e = 1 \times 10^{18}$ m^{-3}. Here, $T_e = T_i$ and $n_e = n_i$ is assumed.

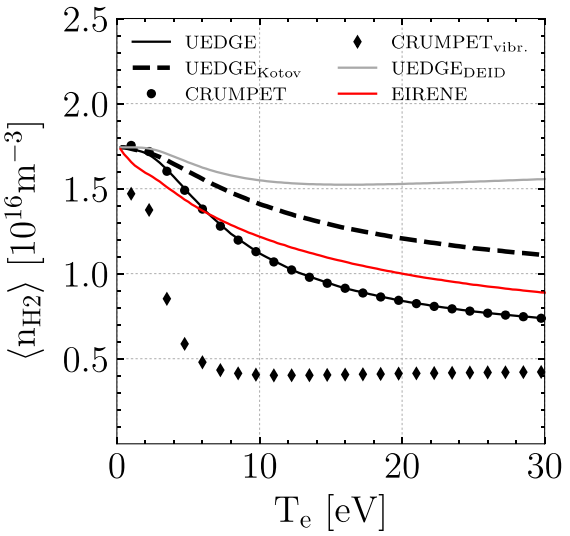

Fig. 6. Comparison of UEDGE (–), using Kotov-2008 rates (– –), UEDGE DEID-only (–), and EIRENE (–) mean H_2 densities for $n_e = 1 \times 10^{18}$ m^{-3}. CRUMPET predictions for H_2 (●) and $H_2(v = 1–14)$ (◆) are also shown. Here, $T_e = T_i$ and $n_e = n_i$ is assumed.

UEDGE over-estimates the mean H_2 density ($\langle n_{H2} \rangle = N_{H2}/V$) by a factor of 10% and 20% at $T_e = 3$ eV and $T_e = 20$ eV, respectively, at $n = 10^{18}$ m^{-3} compared to EIRENE when the Kotov-2008 model, with effective rates calculated by CRUMPET, is used in UEDGE (Fig. 6). Using the Kotov-2008 rates rather than the full set of reactions in Table 1 in UEDGE yields higher $\langle n_{H2} \rangle$ for $T_e > 1.2$ eV due to fewer dissociation reactions being considered. The difference between the UEDGE simulations using Kotov-2008 rates and the EIRENE simulations is attributed to different transport and evaluation of the molecular CRM. The increasing divergence of $\langle n_{H2} \rangle$ with increasing temperature is likely due to elastic scattering, which affects particle transport. EIRENE considers temperature-dependent elastic scattering rates, whereas UEDGE assumes constant elastic scattering rates. As the UEDGE diffusive transport depends on the elastic scattering rates, constant elastic scattering rates are not expected to accurately capture the transition from the fluid regime to the kinetic regime as molecular collisionality decreases, likely under-estimating H_2 transport. Decreased transport out of the domain will result in higher $\langle n_{H2} \rangle$ and increase the transport-time for H_2 to reach the domain boundary. The increased transport-time together with higher $\langle n_{H2} \rangle$ results in a stronger dissociation sink, as observed in Fig. 5. These results are representative of the $n_e = 1 \times 10^{17}$ m^{-3} and $n_e = 1 \times 10^{19}$ m^{-3} simulations.

CRUMPET simulations indicate $H_2(v = 1–14)$ to become significant for $T_e < 6$ eV, as shown by the increase in vibrational population with decreasing temperature (Fig. 6). Here, CRUMPET time-dependently simulates the full computational domain as a single cell to steady-state, without applying the CR approximation, using integrated UEDGE H_2 sinks (transport) and sources (central molecular source) to drive the system. The mean density of the ground state molecules simulated by CRUMPET lie within 4% of the UEDGE predictions, indicating correct implementation of the CR rate coefficients in UEDGE.

The UEDGE simulations using the DEID-only model over-predicts $\langle n_{H2} \rangle$ by a factor up to 1.8 compared to EIRENE due to $\langle \sigma v \rangle_{diss}^{DEID}$ being up to two orders of magnitude smaller than the corresponding Kotov-2008 rate (Fig. 1 and Fig. 6). The nonlinear dependency is due to $S_{diss} \propto n_{H2} \langle \sigma v \rangle_{diss}$.

4. Assessing the molecular energy equation in UEDGE using EIRENE

The same set of simulations was performed in UEDGE using the Kotov-2008 rates as calculated by CRUMPET while evolving the molecular energy equation [21] to assess the agreement with the kinetic model in EIRENE. The UEDGE simulations were performed with flux-limit coefficients $\alpha = 1$ for the H and H_2 particle and energy transport as higher coefficients adversely impacted the numerical stability of the code. The background plasma temperature was decreased from $T_e = 30$ eV until convergence was no longer achieved for each plasma background density. The molecular net energy content in the domain, $E_{H2,tot} = \int(3n_{H2}T_{H2})/2\mathrm{d}V$, is:

$$\frac{dE_{H2,tot}}{dt} = P_{source} + P_{i-H2} + P_{H-H2} - P_{diss} + P_{wall}, \quad (5)$$

where $P_{source} = S_{source}E_{source}$ is the energy influx due to the particle source, $E_{source} = 3T_{source}/2$ the energy of source particles, P_{i-H2} and P_{H-H2} the equipartition between molecules and ions and atoms, respectively, $P_{diss} = |S_{diss}|E_{H2}$ the energy lost due to dissociation of molecules, $E_{H2} = 3T_{H2}/2$ the local molecular energy, and P_{wall} the net energy flux onto the wall [21]. Here, UEDGE assumes $P_{i-H2} + P_{H-H2} = P_{eqp} = \int(3K_{el}n_{H2}(n_i + n_H)(T_i - T_{H2})/2)\mathrm{d}V$ [21], whereas EIRENE only considers ion–molecule scattering: $P_{H-H2} = 0$ W. As the walls are purely absorbing, and the simulations are performed at steady-state $P_{wall} = -P_{source} - P_{eqp} + P_{diss}$ is a sink term (Eq. 5). In EIRENE, $P_{source} = 0.1$ W as the source particles have a defined energy, whereas in UEDGE E_{source} is determined by the local molecular energy and is, thus, coupled to the other terms.

The UEDGE-predicted mean H_2 energy content, $\langle E_{H2}\rangle = E_{H2,tot}/N_{H2}$, (Fig. 7a) is driven by the molecular source P_{source} for $T_e > 5$ eV (Fig. 7b) and by thermal equipartition with ions and atoms P_{eqp} for $T_e < 5$ eV (Fig. 7c). As the domain is small and has absorbing walls, most of the energy supplied by the central source is transported out of the boundary, making P_{wall} the dominant term and $\langle E_{H2}\rangle$ small. However, $\langle E_{H2}\rangle$ displays clear correlation with the volumetric power sinks and sources in the domain. For background plasma density below 1×10^{19} m^{-3} the EIRENE predicts a stronger molecular equipartition source due to scattering with the plasma ions compared to UEDGE, especially for $T_e < 2$ eV (Fig. 7c). This indicates that the constant elastic scattering rate used in UEDGE is lower than predicted by EIRENE, and that a temperature dependent elastic scattering rate should be adopted. For background plasma density 1×10^{19} m^{-3} UEDGE predicts H–H_2 equipartition to become significant, as the UEDGE-predicted molecular equipartition source exceeds that predicted by EIRENE for $T_e > 5$ eV (Fig. 7c). This process, which becomes relevant when n_H becomes comparable to n_{H2} (Fig. 4c) due to stronger dissociation, is not evaluated in the EIRENE simulations and increases P_{eqp}. Both codes predict the molecular dissociation energy sink to be one order of magnitude smaller than the equipartition energy source for background plasma density below 1×10^{19} m^{-3} (Fig. 7d). Only when $n_e = 1 \times 10^{19}$ m^{-3} and $T_e > 5$ eV does the dissociation energy sink become comparable to the molecular equipartition source.

5. The impact of the recycling model on particle balance

The simulations were repeated with background plasma density of 1×10^{18} m^{-3} for a 2D computational domain with three fully recycling carbon walls. The fourth wall is 100% absorbing and a uniform, 1 Ampere-equivalent H_2 wall source was prescribed on the opposite wall. The EIRENE source molecules are prescribed initial energy E = 0.1 eV, whereas $T_{H2} = 0.1$ eV is prescribed throughout the domain and the H_2 energy is not evolved in UEDGE. The EIRENE recycling model is defined by the probabilities of particle reflection (p_f), thermal particle re-emission (p_t) at wall temperature 300 K, and particle absorption (p_a), where $p_f + p_t + p_a = 1$. As the walls are fully recycling $p_a = 0$, the recycling model is controlled by the probability for reflection of H and H_2 (p_f^H and p_f^{H2}, respectively): $p_t = 1 - p_f$. Both H and H_2 are thermally re-emitted as wall-temperature H_2. Here, $p_f^{H2} = 0$ is assumed and $p_f^H \in \{0, f_{TRIM}(\mathbf{v}), 1\}$, where $f_{TRIM}(\mathbf{v})$ is the probability of reflections as a

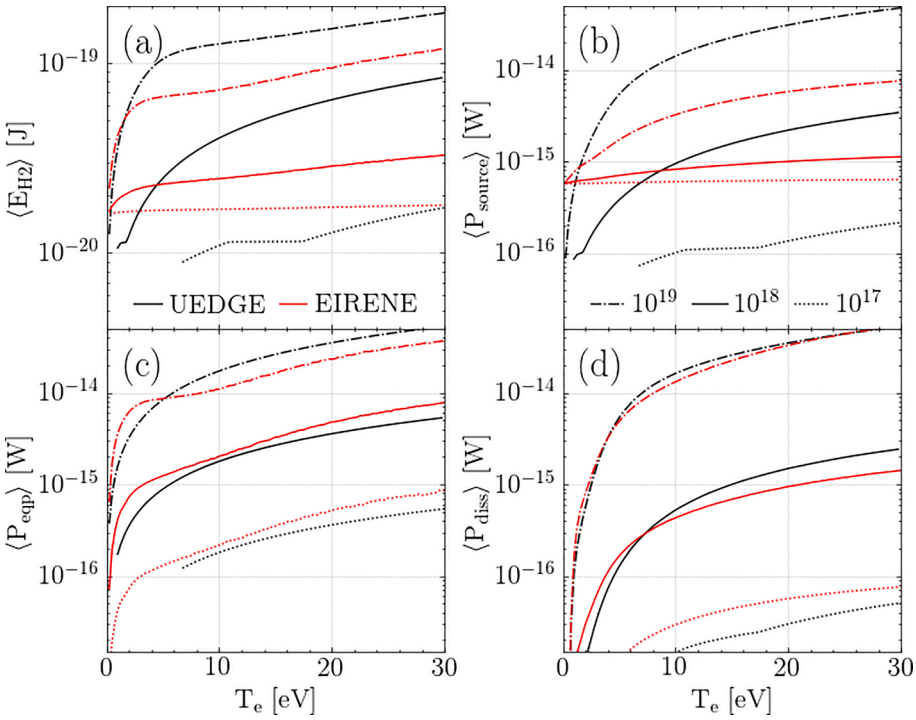

Fig. 7. Mean energy content (a), mean energy source ($\langle P\rangle = P/N_{H2}$) due to the particle source (b), mean thermal equipartition source (c), and mean dissociation energy sink (d) for H_2 predicted by UEDGE (black) and EIRENE (red) for background plasma densities $n_e = 1 \times 10^{17}$ m^{-3} (…), $n_e = 1 \times 10^{18}$ m^{-3} (–), and $n_e = 1 \times 10^{19}$ m^{-3} (–.). Here, $T_e = T_i$ and $n_e = n_i$ is assumed. Note the logarithmic abscissae.

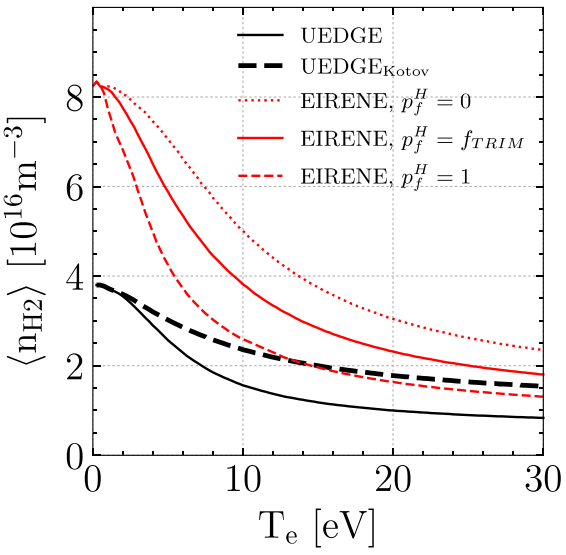

Fig. 8. UEDGE (–), UEDGE using Kotov-2008 rates (– –), and EIRENE with $p_f^H = f_{TRIM}(v)$ (–), $p_f^H = 0$ (...), and $p_f^H = 1$ (– –) for $n_e = 1 \times 10^{18}$ m^{-3}. Here, $T_e = T_i$ and $n_e = n_i$ is assumed.

function on the incident particle velocity according to the TRIM database [22,23]. In terms of wall source strength, $S_{wall}^{pfH=0.} > S_{wall}^{pfH=TRIM} > S_{wall}^{pfH=1} = 0$ s^{-1}. The UEDGE simulations assume all fluxes incident on the walls to be recycled as H_2, corresponding to $p_f^{H2} = 0$, $p_f^H = 0$, and $S_{wall}^{UE} \geq 0$ s^{-1}.

Considering a domain with recycling walls results in $\langle n_{H2} \rangle$ higher by a factor of 2.2 in EIRENE compared to UEDGE as $T_e \to 0$ eV (Fig. 8). As $T_e \to 0$ eV the dissociation sink decreases, $S_{diss} \to 0$ s^{-1}, resulting in higher $\langle n_{H2} \rangle$, which is determined by the rate of transport to the absorbing wall. The EIRENE simulations do not evaluate molecular self-scattering, which increases transport from the source to the absorbing wall, decreasing $\langle n_{H2} \rangle$, explaining why EIRENE predicts higher $\langle n_{H2} \rangle$ than UEDGE as $T_e \to 0$ eV. Furthermore, the uniform wall source results in density gradients, and gradient-driven diffusive transport in UEDGE, towards the absorbing wall only, yielding a greater H_2 flux out of the numerical domain, and subsequently lower $\langle n_{H2} \rangle$, in UEDGE compared to EIRENE.

The UEDGE $\langle n_{H2} \rangle$ predictions are expected to best match the EIRENE $p_f^H = 1$ predictions when the CRUMPET Kotov-2008 rates are used, which occurs as $T_e \to 30$ eV (Fig. 8). The uniform wall source and plasma profiles results in radially uniform H and H_2 distributions and, thus, no diffusive particle transport to the side walls in UEDGE: $S_{wall}^{UE} = 0$ s^{-1}. Hence, the UEDGE simulations are expected to best match the $p_f^H = 1$ EIRENE simulations, which occurs as $T_e \to 30$ eV. EIRENE predicts increasing $\langle n_{H2} \rangle$ with decreasing p_f^H (Fig. 8) as the atoms recycle as molecule at the wall with probability $1 - p_f^H$; consequently, decreasing p_f^H will increase the molecular wall source.

6. Discussion and conclusion

This work demonstrates the implementation of a collisional-radiative (CR) fluid molecular model for hydrogen (H_2) in the edge-fluid code UEDGE, as verified by the kinetic neutral code EIRENE. The fluid molecular model uses effective collisional-radiative reaction rate coefficients calculated by the novel Python tool CRUMPET from, amongst other, the AMJUEL and H2VIBR databases, developed for and used by EIRENE. By using a CR treatment of molecular processes, UEDGE can assess the impact of molecular-assisted processes, such as MAR, MAD, and MAI, molecular binding energy, and molecule-induced radiation on divertor plasmas, which was not possible using the previous molecular model. The implementation of the CR molecular model in UEDGE is expected to improve code-experiment agreement under detached conditions, as all of the aforementioned processes are postulated to play a role in divertor detachment. By using CRUMPET, UEDGE simulations can be post-processed, producing additional atomic and molecular data, such as emission spectra that can be compared to measurements. Here, CRUMPET post-processing of the UEDGE results indicate that the population of vibrationally excited molecules become comparable to the molecular ground state for $T_e = T_i < 6$ eV. Thus, the most important vibrational states should be identified and simulated time-dependently in future versions of the fluid molecular model.

Comparisons between the UEDGE–CRUMPET fluid molecular model and the EIRENE kinetic molecular model show that the agreement of molecular density in a simple, 2D, orthogonal geometry with constant, static plasma profiles is subject to the reactions included in the CR molecular model. When corresponding molecular rate coefficients were used for both codes, agreement for molecular density within 20% was achieved between UEDGE and EIRENE. The equipartition energy source considered in the UEDGE molecular energy equation was found to be up to a factor of 2.1 smaller than that predicted by EIRENE for plasma temperatures below 5 eV, calling for an update of the UEDGE elastic scattering rate coefficient to better correspond to the temperature-dependent behavior observed in EIRENE. When the background plasma density increased beyond 1×10^{19} m^{-3}, UEDGE predicted an increase in thermal equipartition and thermal transport out of the domain that was not observed in EIRENE. The increase in the equipartition source is due to atom-molecule scattering, which is not considered in the EIRENE model used. The comparison also highlighted the impact of recycling on molecular density: the molecular density predicted by EIRENE increased as the fraction reflected molecules decrease, whereas the molecular source from recycled atoms is negligible in UEDGE, due to the absence of radial gradients, which drive the radial diffusive transport in UEDGE. EIRENE predicts a factor of 2.2 higher molecular densities compared to UEDGE for $T_e = T_i \to 0$ eV due to the absence of molecular self-scattering in the EIRENE simulations, which is expected to enhance transport out of the domain at the fluid limit. Further studies assessing more complicated geometries and plasma profiles are necessary to validate the UEDGE recycling model against EIRENE with molecular-self scattering activated.

Additional molecular processes, such as reverse processes, excitation to higher electronic levels, vibrationally resolved excited electronic states, and rotationally resolved reaction rates should be included in CRUMPET for completeness of the collisional-radiative model, but are subject to availability of data. By developing synthetic diagnostics in UEDGE–CRUMPET, the code predictions could be compared to dedicated code-verification experiments in linear machines and tokamaks. By post processing the UEDGE simulations using CRUMPET, synthetic spectra could be compared to the molecular spectra measured in e.g. DIII–D to assess the validity of the molecular fluid model and identify the most important molecular processes. Conversely, CRUMPET could also be used to derive plasma parameters, such as the electron temperature and density, from spectroscopic measurements which, in turn, could be compared to code-experiments.

Declaration of Competing Interest

The authors declare that they have no known competing financial interests or personal relationships that could have appeared to influence the work reported in this paper.

Acknowledgments

The author would like to thank Eric Meier of Zap Energy Inc. and Darren Stotler of Princeton Plasma Physics Laboratory for the private communication that has enabled this work.

This work was performed by LLNL under Contract DE-AC52-07NA27344 and was also supported by the Fulbright Finland Foundation, the Walter Ahlström Foundation, Svensk-Österbottniska Samfundet, Svenska Tekniska Vetenskapsakademien i Finland, the Foundation for Aalto University Science and Technology, Waldemar von Frenckell's Foundation, and Academy of Finland grant agreement No 285143.

References

[1] S. Brezinsek, P.T. Greenland, P.h. Mertens, A. Pospieszczyk, D. Reiter, U. Samm, B. Schweer, G. Sergienko, On the measurement of molecular particle fluxes in fusion boundary plasmas, Journal of Nuclear Materials 313-316 (2003) 967–971, https://doi.org/10.1016/S0022-3115(02)01421-6.

[2] D. Eldon, E. Kolemen, J.L. Barton, A.R. Briesemeister, D.A. Humphreys, A. W. Leonard, R. Maingi, M.A. Makowski, A.G. McLean, A.L. Moser, P.C. Stangeby, Controlling marginally detached divertor plasmas, Nucl. Fusion 57 (6) (2017) 066039, https://doi.org/10.1088/1741-4326/aa6b16.

[3] U. Fantz, "Molecular Diagnostics of Cold Edge Plasmas", in *Nuclear Fusion Research*, Springer-Verlag, Berlin Heidelberg New York, 2005, pp. 99–120.

[4] A.Y. Pigarov, Collisional Radiative Kinetics of Molecular Assisted Recombination in Edge Plasmas, Physica Scripta T96 (1) (2002) 16, https://doi.org/10.1238/Physica.Topical.096a00016.

[5] D. Reiter, M. Baelmans, P. Börner, The EIRENE and B2-EIRENE Codes, Fusion Science and Technology 47 (2) (2005) 172–186, https://doi.org/10.13182/FST47-172.

[6] D. Stotler, R. Kanzleiter, and S. Jaishankar, "User's Guide for DEGAS 2," Princeton, NJ, USA, 2013. [Online]. Available: https://w3.pppl.gov/degas2/.

[7] N. Horsten, W. Dekeyser, M. Blommaert, G. Samaey, M. Baelmans, A hybrid fluid–kinetic neutral model based on a micro–macro decomposition in the SOLPS-ITER plasma edge code suite, Contributions to Plasma Physics 60 (5–6) (2020) 1–7, https://doi.org/10.1002/ctpp.201900132.

[8] T. D. Rognlien and M. E. Rensink, "Users manual for the UEDGE edge-plasma transport code," LLNL Report, 2017. http://github.com/LLNL/UEDGE (accessed May 31, 2020).

[9] P.T. Greenland, Collisional – radiative models with molecules, Proc. R. Soc. Lond. A 457 (2001) 1821–1839.

[10] P.T. Greenland, On the validity of collisional–radiative models, Journal of Nuclear Materials 290-293 (2001) 615–618, https://doi.org/10.1016/S0022-3115(00)00601-2.

[11] A. Holm, Collisional-Radiative UEDGE Model for Plasma Edge Theory (CRUMPET), (accessed Jul. 28 (2020) 2020).

[12] P.T. Greenland, The CRMOL Manual: Collisional Radiative Models for Molecular Hydrogen in Plasmas. (2001).

[13] D. Reiter, "The data file HYDHEL: Atomic and Molecular Data for EIRENE," Jülich, Germany, 2018. [Online]. Available: http://www.eirene.de/html/hydhel.html.

[14] D. Reiter, "The data file H2VIBR: Additional Additional Molecular Data for EIRENE: vibrationally resolved H2(X) ground state," Jülich, Germany, 2017. [Online]. Available: http://www.eirene.de/html/h2vibr.html.

[15] R.K. Janev, J.J. Smith, Cross Sections for Collisions Processes of Hydrogen Atoms with Electrons, Protons and Multiply Charged Ions, vol. 4, International Atomic Energy Agency, Vienna, 1993.

[16] K. Sawada, T. Fujimoto, Effective ionization and dissociation rate coefficients of molecular hydrogen in plasma, Journal of Applied Physics 78 (5) (1995) 2913–2924, https://doi.org/10.1063/1.360037.

[17] U. Fantz, D. Wünderlich, Franck–Condon factors, transition probabilities, and radiative lifetimes for hydrogen molecules and their isotopomeres, Atomic Data and Nuclear Data Tables 92 (6) (2006) 853–973, https://doi.org/10.1016/j.adt.2006.05.001.

[18] D. Reiter, "The data file AMJUEL : Additional Atomic and Molecular Data for EIRENE," Jülich, Germany, 2017. [Online]. Available: http://www.eirene.de/html/amjuel.html.

[19] R. K. Janev, W. D. Langer, K. Evans, and D. E. Post, Elementary Proceses in Hydrogen-Helium Plasmas, First edit., vol. 53, no. 9. London Paris Tokyo: Springer-Verlag Berlin Heidelberg New York, 1987.

[20] V. Kotov, D. Reiter, R.A. Pitts, S. Jachmich, A. Huber, D.P. Coster, Numerical modelling of high density JET divertor plasma with the SOLPS4.2 (B2-EIRENE) code, Plasma Phys. Control. Fusion 50 (10) (2008) 105012, https://doi.org/10.1088/0741-3335/50/10/105012.

[21] A. Holm, T.D. Rognlien, W.H. Meyer, Implementation and assessment of an extended hydrogenic molecular model in UEDGE, Contributions to Plasma Physics (2020), https://doi.org/10.1002/ctpp.201900150.

[22] G. Bateman, "Distribution of neutrals scattered off a wall", Princeton, NJ, USA (1980), https://doi.org/10.1038/283906b0.

[23] W. Eckstein, D.B. Heifetz, Data Sets for Hydrogen Reflection and their Use in Neutral Transport Calculations, Garching bei München (1986).